TRENDS IN STATIC AND DYNAMIC MIXED-MODE FRACTURE

M. Manoharan
Nanotechnology Program
Ceramics and Metallurgy Technologies
GE Global Research
Niskayuna, NY – 12309
USA

ABSTRACT

The last two decades have seen a considerable increase in the amount of research in mixed-mode fracture. This has been driven by a growing realization that in many materials mixed-mode fracture poses a design challenge since the material fails at a lower energy under combined tensile-shear loads than it would under a pure tensile load. Fracture mechanism maps have been proposed to rationalize these trends and delineate regions of susceptibility to mixed-mode fracture. In this paper, these maps will be examined in light of data from a 6061 aluminum alloy tested under two different heat treatments, representing two extreme levels of ductility. The alloy was tested under impact loading conditions and the results compared to earlier work under slow strain rate tests. For very ductile tempers, the imposition of mixed-mode loading further enhances the inherently present shear localization in the deformation ahead of the crack tip. This tends to reduce the overall fracture toughness in the case of the very ductile fully annealed temper. The appearance of sheared dimples in the fracture surface also supports this mechanism. In the case of the peak aged temper, the failure is governed more by the linking up of the primary voids formed at the aging precipitates. In this case, imposition of mixed mode loads leads primarily to redundant work and contributes little to the void formation process. These results are in consonance with the concept of the fracture mechanism map that was originally proposed for explaining trends in mixed-mode fracture under slow strain rates. Thus, the mixed-mode fracture mechanism map is shown to have a wide range of applicability in terms of both the materials and the strain rates involved.

1 INTRODUCTION

A considerable amount of work on mixed mode I/III fracture toughness of materials is available using proportional loading methods (Scroth[1], Manoharan [2], [3], [4], [5], Kumar[6], Gordon[7], Li[8], Manoharan[9], Suresh[10], Manoharan[11], Kamat[12], Manoharan[13]) and all the work using such a loading method has recently been summarized (Manoharan[14]). The superposition of mode III loading results in drastic reduction in fracture toughness in some materials whereas in other materials it has little effect or even results in an increase in the fracture toughness. Fracture mechanism maps delineating regions of susceptibility to tensile and shear loads have been proposed to explain such differences (Manoharan[11], [14]).

In the mixed mode fracture toughness tests outlined above, the use of a modified compact tension specimen has enabled the testing of materials under a variety of combinations of mode I and mode III loadings. By using appropriately defined mixed - mode versions of the stress intensity factor K and the J integral, the susceptibility of these materials to mixed - mode fracture can be quantified. It would be useful to determine if similar results are obtained under dynamic fracture conditions.

2 EXPERIMENTAL PROCEDURES

2.1 Mixed - mode Impact Tests

For evaluating mixed-mode impact behavior, a modified charpy test specimen, shown in Figure 1 was used. The crack inclination angle, θ, can be varied to provide a range of mode I and mode III load combinations. Four angles, 90^o, 75^o, 60^o and 45^o were used. This modified charpy test specimen provides for a simple method to determine the mixed mode impact resistance of materials. Apart from providing information on dynamic fracture under mixed mode conditions, this method could also be potentially used to screen materials quickly for their mixed mode fracture susceptibility. This is especially true in industrial settings where charpy impact tests are routinely used as quality control and analysis tools.

2.2 Materials Studied

The behavior of 6061 aluminum alloy was evaluated under two heat treatment conditions. The peak aged condition was chosen to provide the maximum strength and the fully annealed condition was chosen for maximum ductility / toughness. To obtain the peak aged condition, the alloy was solutionized at 530^oC for 4 hours followed by artificial aging at 177^oC for 8 hours. The fully annealed sample was obtained by heating the specimens for 3 hours at 415^oC.

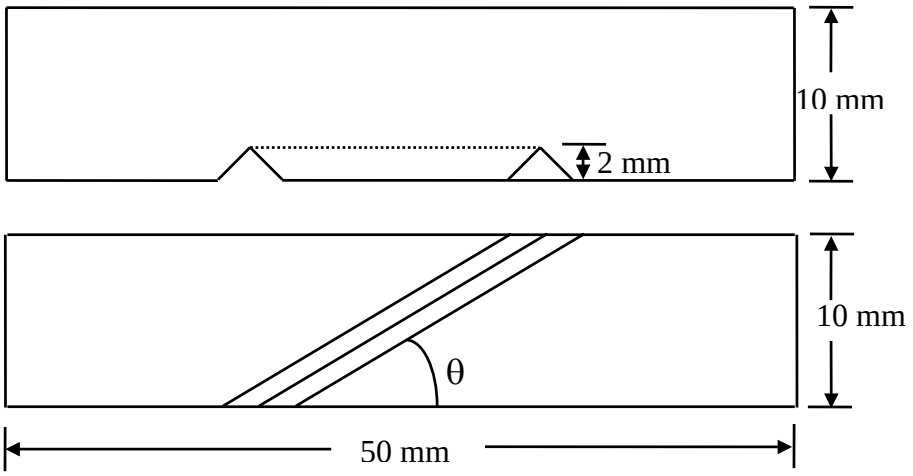

Figure 1 : A Mixed-mode Charpy Impact Specimen

3 RESULTS AND DISCUSSION

3.1 A Mixed-mode Fracture Mechanism Map

The effect of the yield strength and mode I fracture toughness on the mixed-mode fracture toughness can be represented by a plot of J_{Tc} / J_{Ic} versus J_{Ic} / σ_y as shown in Figure 2

(Manoharan[14]). In this plot J_{Tc} refers to the total energy absorbed under combined mode I/III loading, J_{Ic} is the mode I fracture toughness and σ_y is the yield strength of the material. The various materials that make up this plot are also summarized in the reference cited above and include a range of steels, aluminum alloys, ceramics and metal matrix composites (Manoharan[14]). It can clearly be seen that materials which have a very low J_{Ic} / σ_y ratio exhibit a higher mixed-mode fracture toughness than mode I fracture toughness. With an increase in the J_{Ic} / σ_y ratio, the J_{Tc} / J_{Ic} ratio decreases and becomes significantly lower than unity indicating an increased susceptibility to mixed-mode fracture. This trend, however, is reversed after a critical value of J_{Ic} / σ_y is reached. An increase in the J_{Ic} / σ_y ratio beyond this critical value results in an increase in the J_{Tc} / J_{Ic} value and this ratio eventually becomes greater than unity for large J_{Ic} / σ_y values.

The differing susceptibilities of the materials to mixed-mode loading is related to the microstructural fracture mechanisms operative in these materials. Materials with a very low mode I fracture toughness fail predominantly by a cleavage failure process in the case of metallic materials. In the case of the particulate reinforced metal matrix composites, the overall fracture occurs through rapid crack propagation though the local failure mechanism is void nucleation and coalescence. In these materials, the reinforcements crack and act as void nucleation sites under pure mode I loading. However, in these materials, since the failure is by unstable crack propagation, there is not much scope for shear localization to limit the mode I flow field. Hence the mixed-mode fracture toughness is more or less similar to the mode I fracture toughness for these cases. In materials with a higher mode I fracture toughness, the microscopic processes of void nucleation and growth continue to occur. In addition, the crack growth in these materials is stable. The mode III field produces a localized flow on the trajectory of the crack plane ahead of the crack tip. The presence of the voids ahead of the tip limits the region of intense mode I plastic flow, leading to less plastic work dissipation and consequently a decrease in the resolved mode I fracture toughness and the total fracture toughness. Thus the shear mode provides a preferential energy dissipation mechanism in these materials.

A detailed elastic-plastic analysis of the deformation fields in the crack tip region and the effect of the frictional forces, decohered and cracked particles is extremely complex and beyond the capability of current computational capabilities. However, it is significant to note that a wide range of materials can be classified on the basis of their shear susceptibility using the concept of the fracture mechanism map discussed above. The practical guideline which emerges is that materials which show stable ductile fracture governed by voids forming around fine second phase particles are susceptible to shear localization effects and hence mixed mode fracture toughness emerges as an important factor for this class of materials.

3.2 Impact Tests

The total energy absorbed in the impact tests was measured and then normalized by the energy absorbed by the pure Mode I (i.e. standard charpy) specimen. The energy absorbed by the specimens with other crack inclination angles was also normalized with respect to the increased crack width as the crack inclination decreased from 90^o. The results are plotted in Figure 3.

It can be seen from Figure 3 that the behavior of the 6061 aluminum alloy was very different for the two heat treatments studied. While the total energy absorbed increases for the peak aged condition as a function of the crack inclination angle, it decreases as a function of the crack inclination angle for the fully annealed condition. This implies that the addition of mode III loads to the system contributes redundant work in the case of the peak aged alloy while it provides an alternate fracture mechanism in the case of the fully annealed alloy.

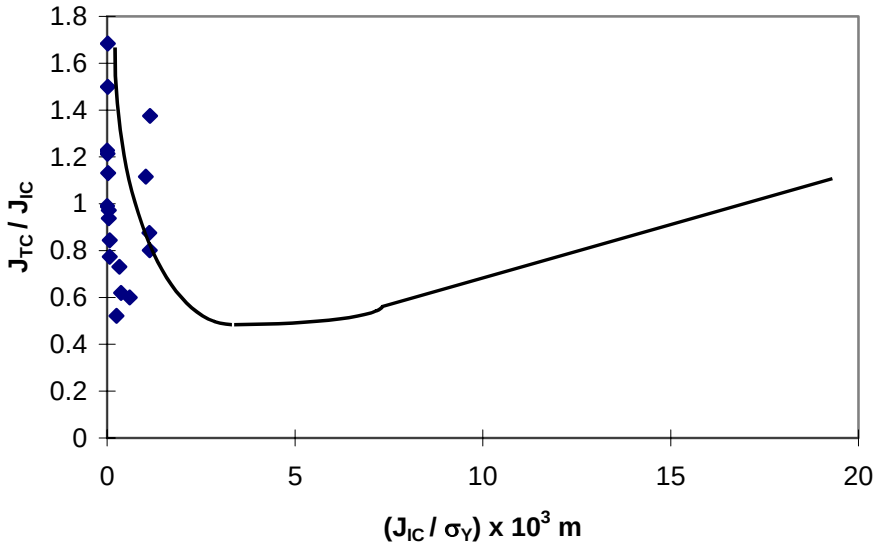

Figure 2 : J_{Tc} / J_{Ic} versus J_{Ic} / σ_y for different materials for a crack inclination angle of 45^o.

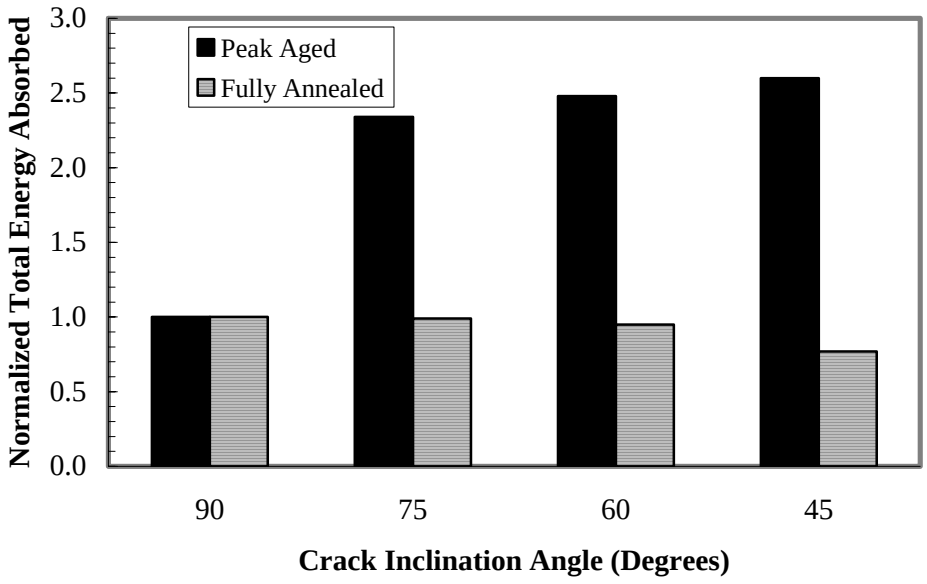

Figure 3 : Normalized total energy absorbed vs. crack inclination angle showing the differences between peak aged and annealed conditions.

The micrographs shown in Figures 4 and 5 also support the conclusions drawn from the impact energy measurements. It can be seen that for the case of the fully annealed material, under pure Mode I loading conditions, the dimples are equiaxed, though some evidence of localized shearing is apparent. Under mixed-mode loading conditions, when the crack inclination angle is 45^o, the dimples are very elongated and smeared out, indicating the overwhelming effect of the imposed shear. In the case of the peak aged material, the fractograph shows predominantly equiaxed dimples for pure Mode I loading. When Mode III loads are added and the value of the crack inclination angle is 45^o, the dimples continue to be equiaxed.

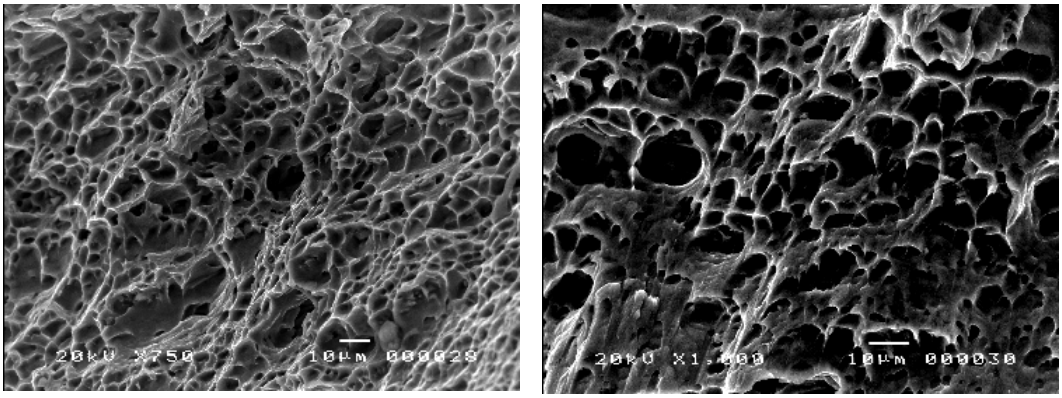

Figure 4 : Mode I (Left) and Mixed-Mode I/III (Right) Fracture Surfaces in Annealed Condition

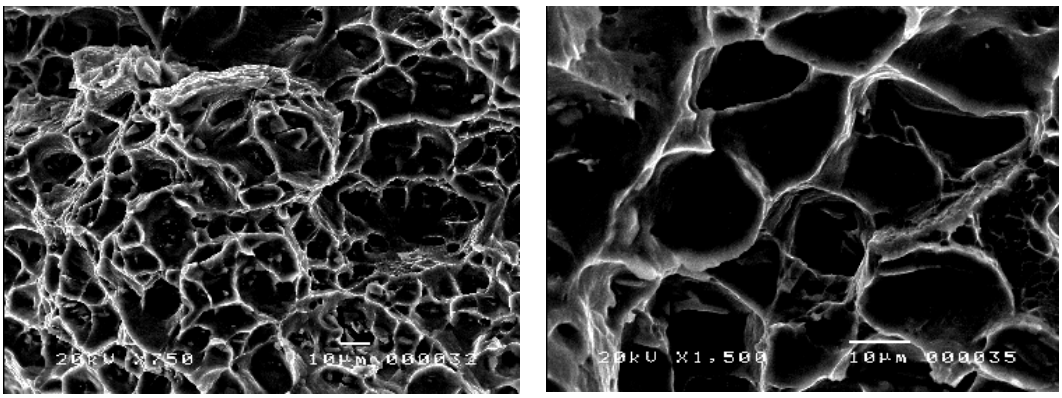

Figure 5 : Mode I (Left) and Mixed-Mode I/III (Right) Fracture Surfaces in Peak Aged Condition

This behavior is consistent with the concept of a fracture mechanism map as discussed earlier. In essence, as the mode I fracture toughness increases the susceptibility to mixed-mode fracture also increases. For very ductile tempers, the imposition of mixed-mode loading further enhances the inherently present shear localization in the deformation ahead of the crack tip. This tends to reduce the overall fracture toughness as is the case for the very ductile fully annealed temper. The appearance of the fracture surface also supports this mechanism. In the case of the peak aged

temper, the failure is governed more by the linking up of the primary voids formed at the aging precipitates. In this case, imposition of mixed mode loads leads primarily to redundant work and contributes little to the void formation process.

The current set of experiments using a modified charpy specimen indicate that the above concepts developed primarily for slow strain rate fracture toughness tests are in principle extendible to the case of dynamic impact fracture. Studies on steels above and below the ductile - brittle transition temperature also indicate similar trends. Thus the use of the modified charpy specimen can be considered to test the impact fracture resistance of materials under mixed-mode loading conditions, where shear mechanisms may represent alternate lower energy processes.

4 REFERENCES

1. J.G. Schroth, J.P. Hirth, R.G. Hoagland and A.R. Rosenfield, Metallurgical Transcactions 18A, 1061, (1987).
2. M. Manoharan, J.P. Hirth and A.R. Rosenfield, Scripta Metallurgica 23, 763, (1989).
3. M. Manoharan, S. Raghavachary, J.P. Hirth and A.R. Rosenfield, Journal of Engineering Materials Technology 111, 440, (1989).
4. M. Manoharan, J.P. Hirth and A.R. Rosenfield, Acta Metallurgica et Materialia 39, 1203, (1991).
5. M. Manoharan, J.P. Hirth and A.R. Rosenfield, Journal of Testing and Evaluation 18, 106, (1990).
6. A.M. Kumar and J.P. Hirth, Scripta Metallurgica et Materialia 25, 985, (1991).
7. J.A. Gordon, J.P. Hirth, A.M. Kumar and N. E. Moody, Metallurgical Transactions 23A, 1013, (1992).
8. H. Li, H. Jones, J.P. Hirth and D.S. Gelles, Journal of Nuclear Materials 215, 741, (1994).
9. M. Manoharan, Journal of Materials Science Letters, 15, 254, (1996).
10. S.Suresh and E.K. Tschegg, Journal of American Ceramic Society 70, 726, (1989).
11. M. Manoharan, Scripta Metallurgica et Materialia 26, 1187, (1992).
12. S.V. Kamat and J.P. Hirth, Scripta Metallurgica et Materialia, 30, 145, (1994).
13. M. Manoharan and J.J. Lewandowski, Journal of Composite Materials, 25, 831, (1991).
14. M. Manoharan and S.V. Kamat, International Journal of Fracture, 73, R41, (1996).